SAND2017-10729J

Experimental Determination of Solubilities of Magnesium Borates: Solubility Constants of Boracite [$Mg_3B_7O_{13}Cl$(cr)] and Aksaite [$MgB_6O_7(OH)_6 \cdot 2H_2O$(cr)]

Yongliang Xiong[1], Leslie Kirkes, Jandi Knox, Cassie Marrs, and Heather Burton

Sandia National Laboratories (SNL)*
Carlsbad Programs Group
4100 National Parks Highway, Carlsbad, NM 88220, USA

[1] Corresponding author, e-mail: yxiong@sandia.gov.

ABSTRACT

In this study, solubility measurements regarding boracite [$Mg_3B_7O_{13}Cl$(cr)] and aksaite [$MgB_6O_7(OH)_6{\bullet}2H_2O$(cr)] from the direction of supersaturation were conducted at 22.5 ± 0.5°C. The equilibrium constant ($\log_{10} K^0$) for boracite in terms of the following reaction,

$$Mg_3B_7O_{13}Cl(cr) + 15H_2O(l) \rightleftharpoons 3Mg^{2+} + 7B(OH)_4^- + Cl^- + 2H^+$$

is determined as –29.49 ± 0.39 (2σ) in this study.

The equilibrium constant for aksaite according to the following reaction,

$$MgB_6O_7(OH)_6{\bullet}2H_2O(cr) + 9H_2O(l) \rightleftharpoons Mg^{2+} + 6B(OH)_4^- + 4H^+$$

is determined as –44.41 ± 0.41 (2σ) in this work.

This work recommends a complete set of thermodynamic properties for aksaite at 25°C and 1 bar as follows: ΔH_f^0 = –6063.70 ± 4.85 kJ•mol^{-1}, ΔG_f^0 = –5492.55 ± 2.32 kJ•mol^{-1}, and S^0 = 344.62 ± 1.85 J•mol^{-1}•K^{-1}. Among them, ΔG_f^0 is derived from the equilibrium constant for aksaite determined by this study; ΔH_f^0 is from the literature, determined by calorimetry; and S^0 is computed in the present work from ΔG_f^0 and ΔH_f^0.

This investigation also recommends a complete set of thermodynamic properties for boracite at 25°C and 1 bar as follows: $\Delta H_f^0 = -6575.02 \pm 2.25$ kJ•mol^{-1}, $\Delta G_f^0 = -6178.35 \pm 2.25$ kJ•mol^{-1}, and $S^0 = 253.6 \pm 0.5$ J•mol^{-1}•K^{-1}. Among them, ΔG_f^0 is derived from the equilibrium constant for boracite determined by this study; S^0 is from the literature, determined by calorimetry; and ΔH_f^0 is computed in this work from ΔG_f^0 and S^0.

The thermodynamic properties determined in this study can find applications in many fields. For instance, in the field of material science, boracite has many useful properties including ferroelectric and ferroelastic properties. The equilibrium constant of boracite determined in this work will provide guidance for economic synthesis of boracite in an aqueous medium. Similarly, in the field of nuclear waste management, iodide boracite [$Mg_3B_7O_{13}I$(cr)] is proposed as a waste form for radioactive ^{129}I. Therefore, the solubility constant for chloride boracite [$Mg_3B_7O_{13}Cl$(cr)] will provide the guidance for the performance of iodide boracite in geological repositories. Boracite/aksaite themselves in geological repositories in salt formations may be solubility-controlling phase(s) for borate. Consequently, solubility constants of boracite and aksaite will enable researchers to predict borate concentrations in equilibrium with boracite/aksaite in salt formations.

INTRODUCTION

Boracites with a general formula $M_3B_7O_{13}X$ (M = Mg, and transition elements Cr, Mn, Fe, Co, Ni, Cu, Zn, or Cd; X = halide, F, Cl., Br, or I) constitute a large group of

55 isomorphous compounds with more than 20 species (Li et al., 2003). Among them, the
56 boracite end member with Mg and Cl., i.e., $Mg_3B_7O_{13}Cl$, is an important borate mineral.
57 (In the following, unless otherwise noted, boracite refers to the end member with Mg and
58 Cl for simplicity.) It occurs in evaporate deposits in salt formations (e.g., Phillips, 1947;
59 Green, 2010; Gao, et al., 2012; Zhang et al., 2013), and the description about its
60 occurrence appeared in the literature as early as in the nineteen century (Magtear, 1869;
61 Cadell, 1885), and it is also present in salt lakes (e.g., Heggemann et al., 1994; Zheng,
62 1997). In the field of material science, boracites have many useful properties including
63 ferroelectric and ferroelastic properties (e.g., Torre et al., 1972).
64 Aksaite with a structural formula of $MgB_6O_7(OH)_6 \cdot 2H_2O$(cr) is a magnesium
65 borate mineral, which was discovered in 1960's (Clark and Erd, 1963; Dal Negro et al.,
66 1971). It is also present in evaporate deposits in salt formations (Valeyev et al., 1973;
67 Garrett, 1998), and in salt lakes (Li et al., 2012).
68 In the field of nuclear waste management, as boracite and aksaite are present in
69 evaporate deposits in salt formations mentioned before, they are potentially important to
70 geological repositories in salt formations. Salt formations are considered to be ideal for
71 nuclear waste isolation (National Academy of Science, 1957). Recent investigations
72 have suggested that borate could potentially complex with Nd(III) (Borkowski et al.,
73 2010; Xiong, 2017), an analog to Am(III) in chemical behavior. Hence, a comprehensive
74 understanding of interactions of borate with major ions in brines as well as the potential
75 solubility-controlling phase(s) for borate is needed to accurately describe the
76 contributions of borate to the potential solubility of Am(III) in brines in salt formations,
77 as they contain significant concentrations of borate. In brines associated with salt

formations, they contain high concentrations of chloride along with significant concentrations of boron and magnesium. For instance, at the Waste Isolation Pilot Plant (WIPP), a U.S. Department of Energy geological repository for the permanent disposal of defense-related transuranic (TRU) waste (U.S. DOE, 1996), the Generic Weep Brine (GWB) and Energy Research and Development Administration Well 6 (ERDA-6), contain high concentrations of chloride, borate and magnesium (Xiong and Lord, 2008). Consequently, in geological repositories in salt formations, the interactions among chloride, borate, and magnesium, will be important to the accurate description of the contributions of borate to the solubility of Am(III) in brines in salt formations.

In addition, iodide-boracites, ($M_3B_7O_{13}I$, where *M* represents various divalent metal ions), have been proposed as a waste form for radioactive iodine, ^{129}I, in the field of nuclear waste management (e.g., Vance et al., 1981).

Thermodynamic properties of boracite is not well known. Anovitz and Hemingway (2002) listed the Gibbs free energy of formation for boracite from an unpublished source from Khodakovsky, Semenov and Aksaenova (see Page 196, 252 in Anovitz and Hemingway, 2002). Regarding aksaite, Jia et al. (1999) determined its enthalpy of formation using the calorimetric method. However, its Gibbs free energy of formation has not been determined, and therefore its solubility constant is unknown. The knowledge of the complete sets of thermodynamic properties for aksaite and boracite will be useful to many fields. For this reason, in this work, we determine the solubility constants of boracite and aksaite. Then, based on our solubility constants, we are able to provide the complete sets of thermodynamic properties for aksaite and boracite.

EXPERIMENTAL METHODS

In our solubility experiments, we performed the solubility measurements from the direction of supersaturation. All chemicals used in our experiment were ACS reagent grade.

In our supersaturation experiment, we first placed 250 mL of a 1.0 $mol \bullet kg^{-1}$ $MgCl_2$ solution into a glass beaker with a stir bar. Then, 8.5023 grams of H_3BO_3 was added into the above solution. The solution was well mixed until all of H_3BO_3 was dissolved. After that, 2.0114 $mol \bullet dm^{-3}$ NaOH was dropwise added into the above solution to initiate precipitation. Finally, the solution with precipitates was transferred from the glass beaker into a 500 mL plastic bottle for storage of the supersaturation experiment at 22.5 ± 0.5°C. The experiment was not sampled until the experimental duration lasted at least for 970 days.

The pH readings were measured with an Orion-Ross combination pH glass electrode, coupled with an Orion Research EA 940 pH meter that was calibrated with three pH buffers (pH 4, pH 7, and pH 10). Negative logarithms of hydrogen-ion concentrations on molar scale (pcH) were determined from pH readings by using correction factors (Hansen, 2001). Based on the equation in Xiong et al. (2010), pcHs are converted to negative logarithms of hydrogen-ion concentrations on molal scale, pH_m,. a notation from Oak Ridge National Laboratory/University of Idaho (e.g., Wood et al., 2002).

Solution samples were periodically withdrawn from experimental runs. Before solution samples were taken, pH readings of experimental runs were first measured. The sample size was usually 3 mL. After a solution sample was withdrawn from an

experiment and filtered with a 0.2 μm syringe filter, the filtered solution was then weighed, acidified with 0.5 mL of concentrated TraceMetal® grade HNO_3 from Fisher Scientific, and finally diluted to a volume of 10 mL with DI water. If subsequent dilutions were needed, aliquots were taken from the first dilution samples for the second dilution, and aliquots of the second dilution were then taken for the further dilution.

Boron, sodium and magnesium concentrations of solutions were analyzed with a Perkin Elmer dual-view inductively coupled plasma-atomic emission spectrometer (ICP-AES) (Perkin Elmer DV 8300). Calibration blanks and standards were precisely matched with experimental matrices. The linear correlation coefficients of calibration curves in all measurements were better than 0.9995. The analytical precision for ICP-AES is better than 1.00% in terms of the relative standard deviation (RSD) based on replicate analyses.

Chloride concentrations were analyzed with a DIONEX ion chromatograph (IC) (DIONEX IC 3000).

The solid phase identification was performed by using a Bruker AXS, Inc., D8 Advance X-ray diffractometer (XRD) with a Sol-X detector. XRD patterns were collected using CuKα radiation at a scanning rate of 1.33°/min for a 2θ range of 10–90°.

EXPERIMENTAL RESULTS

Figure 1 shows the XRD patterns for our supersaturation experiment with an initial concentration of 1.0 mol•kg^{-1} $MgCl_2$ solution. Figure 1 shows that boracite along with aksaite crystallized from the solution. Notice that the peaks characteristic of boracite and aksaite, are present in the XRD patterns for our experiment (Figure 1).

Experimental results are tabulated in Table 1. In Figure 2, total boron, chloride, magnesium and sodium concentrations as a function of experimental time are displayed respectively. From Figure 2, we can see that the equilibrium was established after about 900 days. The duration of our experiment was long, and it was up to 1,642 days (Table 1, Figure 2).

THERMODYNAMIC CALCULATIONS, DISCUSSIONS, AND APPLICATIONS

The dissolution reactions for boracite and aksaite, and the equilibrium between boracite and aksaite, can be represented by the following reactions,

$$Mg_3B_7O_{13}Cl(cr) + 15H_2O(l) \rightleftharpoons 3Mg^{2+} + 7B(OH)_4^- + Cl^- + 2H^+ \quad (1)$$

$$MgB_6O_7(OH)_6{\bullet}2H_2O(cr) + 9H_2O(l) \rightleftharpoons Mg^{2+} + 6B(OH)_4^- + 4H^+ \quad (2)$$

$$Mg_3B_7O_{13}Cl(cr) + 10H^+ + 11B(OH)_4^- \rightleftharpoons 3MgB_6O_7(OH)_6{\bullet}2H_2O(cr) + 12H_2O(l) + Cl^- \quad (3)$$

Regarding Reaction (1), its equilibrium constant at infinite dilution can be expressed as follows,

$$K_1^0 = \frac{(a_{Mg^{2+}})^2 \times (a_{B(OH)_4^-})^7 \times (a_{Cl^-}) \times (a_{H^+})^2}{(a_{H_2O})^{15}} \quad (4)$$

Similarly, the equilibrium constant at infinite dilution for Reaction (2) can be cast as follows,

$$K_2^0 = \frac{(a_{Mg^{2+}}) \times (a_{B(OH)_4^-})^6 \times (a_{H^+})^4}{(a_{H_2O})^9} \quad (5)$$

Finally, the equilibrium constant at infinite dilution for Reaction (3) is written as follows,

$$K_3^0 = \frac{(a_{H_2O})^{12} \times (a_{Cl^-})}{(a_{H^+})^{10} \times (a_{B(OH)_4^-})^{11}} \quad (6)$$

In Equations (4) through (6), a_i is an activity of the i-th species calculated with a thermodynamic model; a_{H_2O} activity of water.

Activities of Mg^{2+}, $B(OH)_4^-$, Cl^-, H^+ and water in the experimental system are calculated by using the computer code EQ3/6 Version 8.0a (Wolery et al., 2010; Xiong, 2011a). The database used for calculations was DATA0.FM2 (Xiong and Domski, 2016), which utilizes the Pitzer model for calculations of activity coefficients of aqueous species with updates for borate chemistry from Xiong et al. (2013).

Based on the activities calculated using EQ3/6 Version 8.0a, the $\log K_1^0$ and $\log K_2^0$ at infinite dilution are calculated in accordance with Equations (4) and (5)

188 (Table 2). The equilibrium constant for Reaction (3) can be derived from $\log K_1^0$ and

189 $\log K_2^0$, or calculated from Equation (6).

190 The equilibrium constants for boracite and aksaite determined by this study

191 provide the best opportunity in evaluating the Gibbs free energies of these phases from

192 the unpublished source and estimates in the literature. According to the unpublished

193 source, Khodakosky, Semenov and Aksaenova calculated the ΔG_f^0 of boracite as -6178.4

194 kJ•mol^{-1} (cited in Anovitz and Hemingway, 2002), based on their unpublished

195 calorimetric data for the enthalpy and entropy of boracite. The equilibrium constant

196 ($\log_{10} K^0$) regarding Reaction (1) calculated from the ΔG_f^0 from Khodakosky, Semenov

197 and Aksaenova is –29.50 (Table 3). In the calculations, the Gibbs free energies for other

198 species in Reaction (1) are taken from the NBS Thermodynamic Tables (Wagman et al.,

199 1982), as Anovitz and Hemingway (2002) implied that the thermodynamic properties of

200 boracite from Khodakosky, Semenov and Aksaenova are consistent with the NBS

201 Thermodynamic Tables. In comparison with $\log_{10} K^0$ of –29.50 ± 0.39 determined by

202 this study, the value (–29.50) calculated from the ΔG_f^0 from Khodakosky, Semenov and

203 Aksaenova is in excellent agreement with our value.

204 Anovitz and Hemingway (2002) estimated the ΔG_f^0 of boracite as –6184.7

205 kJ•mol^{-1}. The equilibrium constant in 10-based logarithmic unit calculated from their

206 estimated ΔG_f^0 is –30.61. This value differs from our experimental value by about one

207 order of magnitude.

208 Li et al. (2000) calculated the ΔG_f^0 of aksaite as –5495.64 kJ•mol^{-1}, based on

209 their group contribution method for hydrated borates. The equilibrium constant

($\log_{10} K^0$) regarding Reaction (2) calculated from the ΔG_f^0 from Li et al. (2002) is -44.95 (Table 3). In the calculations, the Gibbs free energies for other species in Reaction (2) are taken from the NBS Thermodynamic Tables (Wagman et al., 1982), as the group contribution method they developed is consistent with the NBS Thermodynamic Tables. Interestingly, this value (–44.95) compares favorably with our experimental value of -44.41 ± 0.41.

Anovitz and Hemingway (2002) estimated the ΔG_f^0 of aksaite as –5569 kJ•mol^{-1}. Based on this value for ΔG_f^0, the equilibrium constant for Reaction (2) is calculated to be –57.81 (Table 3). In the calculations, the Gibbs free energies for other species in Reaction (2) are taken from the NBS Thermodynamic Tables (Wagman et al., 1982), as the method of Anovitz and Hemingway (2002) was developed based on the database of the NBS Thermodynamic Tables. Obviously, the equilibrium constant (-57.81) for Reaction (2) according to the ΔG_f^0 of aksaite estimated from the method of Anovitz and Hemingway is too low in comparison with our experimental value (-44.41 ± 0.41) and the value (-44.95) calculated from the ΔG_f^0 from Li et al. (2000).

In accordance with the equilibrium constants for boracite and aksaite determined in this study, we recommend the complete sets of thermodynamic properties for boracite and aksaite, in combination with S^0 for boracite from Khodakovsky, Semenov and Aksaenova (cited in Anovitz and Hemingway) and ΔH_f^0 for aksaite from Jia et al. (1999) (Table 4).

Anovitz and Hemingway (2002) estimated the enthalpy (ΔH_f^0) and Gibbs free energy (ΔG_f^0), of formation, for aksaite based on their estimation method. The

232 estimation method of Anovitz and Hemingway (2002) for borates was developed from
233 the approaches of Robinson and Haas (1983), Chermak and Rimstidt (1989), and
234 Hemingway (1982). These approaches are mainly related to silicate minerals.
235 Anovitz and Hemingway (2002) estimated the ΔH_f^0 and ΔG_f^0 of aksaite as –6135
236 kJ•mol^{-1} and –5569 kJ•mol^{-1} (Table 4), respectively.
237 Jia et al. (1999) experimentally determined the ΔH_f^0 of aksaite as –6063.65 ±
238 4.85 kJ•mol^{-1} (Table 4). In comparison, the estimated value provided by
239 Anovitz and Hemingway (2002) differs from the experimental value of Jia et al. (1999)
240 by 71 kJ•mol^{-1}. Li et al. (2000) calculated the ΔH_f^0 of aksaite as –6007.00 kJ•mol^{-1}.
241 The ΔH_f^0 calculated by Li et al. (2000) differs from the experimental value by 56
242 kJ•mol^{-1}. In addition, Li et al. (2000) also calculated the ΔG_f^0 of aksaite to be –5495.64
243 kJ•mol^{-1}. The ΔH_f^0 and ΔG_f^0 values calculated by Li et al. (2000) are based on the
244 group contribution method they developed for hydrated borates. The ΔG_f^0 value
245 estimated by Anovitz and Hemingway (2002) differs from the calculated value of Li et al.
246 (1999) by 73 kJ•mol^{-1}.
247 The ΔG_f^0 of aksaite computed from the equilibrium constant determined in this
248 study is –5492.55 ± 2.32 kJ•mol^{-1}. In the computation, the thermodynamic properties for
249 the species except aksaite in Reaction (2) are taken from the NBS Tables (Wagman et al.,
250 1982). This is done in order to be consistent with the thermodynamic database of
251 Anovitz and Hemingway (2002), Jia et al. (1999), and Li et al. (2002); all of them are
252 consistent with the NBS Tables. It is clear from Table 4 that the ΔG_f^0 value for aksaite

253 derived from the equilibrium constant determined by this work is in very good agreement
254 with that from Li et al. (2000), but differs significantly from that from Anovitz and
255 Hemingway (2002). Therefore, it seems that the method of Li et al. (2000) is more
256 reliable for estimating thermodynamic properties of hydrated borates.

257 In summary, the equilibrium constant for boracite determined by this study is in
258 excellent agreement with the ΔG_f^0 derived from the calorimetric measurements, from
259 Khodakovsky, Semenov and Aksaenova. The equilibrium constant for aksaite
260 determined in this work is in close agreement with the ΔG_f^0 calculated from the group
261 contribution method (Li et al., 2002). The good agreement between the equilibrium
262 measurements and calorimetric measurements for boracite also provides the additional
263 credits and independent validation for the aqueous chemistry model including borate
264 species that has been employed for equilibrium calculations.

265 The complete sets of thermodynamic properties for boracite and aksaite may find
266 applications in many fields. For instance, aksaite double salt has been observed in Da
267 Chaidam Salt Lake and Xiao Chaidam Salt Lake (Li et al., 2012). Therefore, the
268 thermodynamic properties of aksaite can be used to elucidate the conditions for the
269 formation of aksaite in those salt lakes, including temperature variations.

270 Boracite appears in salt formations in various assemblages. In the salt formation
271 in the Khorat basin in Thailand, boracite co-exists with carnallite ($KMgCl_3 \cdot 6H_2O$) and
272 bischofite ($MgCl_2 \cdot 6H_2O$) (Le, 1986).

273

SUMMARY

In this study, the equilibrium constants for boracite and aksaite have been determined in supersaturation experiments. The equilibrium constant for boracite obtained in this study based on the equilibrium aqueous chemistry model including borate species is in excellent agreement with the value calculated from the thermodynamic properties of boracite determined by Khodakovsky, Semenov and Aksaenova using the calorimetric method. The equilibrium constant for aksaite determined in this work is also in close agreement with the ΔG_f^0 calculated from the group contribution method (Li et al., 2002). Therefore, our equilibrium measurements are consistent with the calorimetric measurement.

Based on our equilibrium measurements, we recommend the complete sets of thermodynamic properties for boracite and aksaite, which are consistent with the calorimetric measurements.

ACNOWLEDGEMENTS

Sandia National Laboratories is a multimission laboratory operated by National Technology and Engineering Solutions of Sandia, LLC., a wholly owned subsidiary of Honeywell International, Inc., for the U.S. Department of Energy's National Nuclear Security Administration under contract DE-NA-0003525. This research is funded by WIPP programs administered by the Office of Environmental Management (EM) of the U.S Department of Energy. We are grateful to Shelly Nielsen, Lindsay Day, Diana Goulding, Brittany Hoard, Chase Kicker, Danelle Morrill, William Sullvan, Mathew Stroble, Kira Vincent, and Yoni Xiong for their laboratory assistance.

299 REFERENCES
300
301 Anovitz, L.M., and Hemingway, B.S., 2002. Thermodynamics of boron minerals:
302 Summary of structural, volumetric and thermochemical data. In Grew, E.S., and
303 Anovitz, L.M., Editors, Boron: Mineralogy, Petrology, and Geochemistry, Reviews
304 in Mineralogy, Volume 33, p. 181-262, .2nd Printing, Mineralogical Society of
305 America, Washington, D.C., USA.

306 Borkowski, M., Richmann, M., Reed, D.T., and Xiong, Y.-L. (2010) Complexation of
307 Nd(III) with Tetraborate Ion and Its Effect on Actinide (III) Solubility in WIPP
308 Brine. Radiochimica Acta, 98, 577–582.

309 Braitsch, O., 1971. Other Components of Salt Deposits. In *Salt Deposits Their Origin and*
310 *Composition* (pp. 215-245). Springer Berlin Heidelberg.

311 Cadell, H.M., 1885. The salt deposits of Stassfurt. *Transactions of the Edinburgh*
312 *Geological Society*, *5*(1), pp.92-103.

313 Chermak, J.A., and Rimstidt, J.D., 1989. Estimating the thermodynamic properties
314 (ΔG_f^0 and ΔH_f^0) of silicate minerals at 298 K from the sum of polyhedral
315 contributions. American Mineralogist 74:1023-1031.

316 Clark, J.R. and Erd, R.C., 1963. Probable chemical formula of aksaite, a new hydrated
317 magnesium borate. *American Mineralogist*, *48*(7-8), p.930.

318 Dal Negro, A., Ungaretti, L., and Sabelli, C., 1971. Crystal structure of aksaite.
319 *American Mineralogist*, *56*(9-10), p.1553

320 Garrett, D.E., 1998. *Borates: Handbook of deposits, processing, properties, and use*.
321 Academic Press.

322 Gao, X., Cai, K.Q., Li, D.R., Peng, Q., Fang, Q.F. And Qin, H., 2012. Mineralogical and
323 geochemical characteristics and genesis of the potassium-magnesium salt deposit in
324 Khammouan Province, Laos [J]. *Acta Petrologica Et Mineralogica*, *4*, p.011.

325 Green, D.I. and Freier, M.D., 2010. The Boulby mine. *The Mineralogical Record*, *41*(1),
326 pp.S53-S53.

327 Heggemann, H., Helmcke, D. and Tietze, K.W., 1994. Sedimentary evolution of the
328 Mesozoic Khorat Basin in Thailand. *Zentralblatt für Geologie und Paläontogie, Teil*
329 *I*, pp.11-12.

330 Hemingway, B.S., 1982. Thermodynamic properties of calcium aluminates. Journal of
331 Physical Chemistry 2802-2803.

Jia, Y.-Z, Li, J., Gao, S.-Y., and Xia, S.-P., 1999. Thermochemistry of aksaite. *The Journal of Chemical Thermodynamics*, *31*(12), pp.1605-1608.

Le Thi Hoe (1986): Petrographical character of rocks salt in the Vien- tiane basin, Laos. - Intergeo, GDMG; Vietnam.

Li, J., Li, B. and Gao, S., 2000. Calculation of thermodynamic properties of hydrated borates by group contribution method. *Physics and Chemistry of Minerals*, *27*(5), pp.342-346.

Li, D., Xu, Z.J., Wang, Z.H., Geng, D.Y., Zhang, J.S., Zhang, Z.D., Yuan, G.L. and Liu, J.M., 2003. Synthesis and characterization of M–Cl (M= Fe, Co, Ni) boracites. *Journal of alloys and compounds*, *351*(1), pp.235-240.

Li, X., Liu, Z., Gao, S. and Xia, S., 2012. Geochemical hypothesis for hydrated magnesium borate deposit in Salt Lake, NW China. *Environmental Earth Sciences*, *66*(5), pp.1431-1438.

Li, F., Lin, C.X., Yang, L.J., Guo, Y.F., Wang, S.Q. and Deng, T.L., 2013. Synthesis and Thermodynamic Properties of Magnesium Borates. In *Advanced Materials Research* (Vol. 791, pp. 220-223). Trans Tech Publications.

Magtear, B., 1869. The salt deposits at stassfurt. *Journal of the Franklin Institute*, *87*(6), pp.408-413.

National Academy of Sciences Committee on Waste Disposal. 1957. *The Disposal of Radioactive Waste on Land*. Publication 519. Washington, DC: National Academy of Sciences–National Research Council.

Phillips, F.C., 1947. Oceanic salt deposits. *Quarterly Reviews, Chemical Society*, *1*(1), pp.91-111.

Robinson, G.R., Jr., Haas, J.L., Jr., 1983. Heat capacity, relative enthalpy, and calorimetric entropy of silicate minerals: An empirical method of prediction. American Mineralogist 68:541-553.

Torre, L.P., Abrahams, S.C. and Barns, R.L., 1972. Ferroelectric and ferroelastic properties of Mg-Cl-Boracite. *Ferroelectrics*, *4*(1), pp.291-297.

U.S. DOE (1996) Compliance Certification Application 40 CFR Part 191 Subpart B and C U.S. Department of Energy Waste Isolation Pilot Plant. Appendix SOTERM. DOE/CAO 1996-2184. Carlsbad, NM: U.S. DOE Carlsbad Area Office.

Valeyev, R.N., Ozol, A.A. and Tikhvinskiy, I.N., 1973. Genetic characteristics of the halide-sedimentational type of borate deposits. *International Geology Review*, *15*(2), pp.165-172.

Vance, E.R., Agrawal, D.K., Scheetz, B.E., Pepin, J.G., Atkinson, S.D. and White, W.B., 1981. *Ceramic phases for immobilization of/sup 129/I.[Sodalite and boracite]* (No. DOE/ET/41900-9; ESG-DOE-13354). Rockwell International Corp., Canoga Park, CA (USA). Energy Systems Group; Pennsylvania State Univ., University Park (USA). Materials Research Lab.

Wagman, D.D., Evans, W.H., Parker, V.B., Schumm, R.H. and Halow, I., 1982. *The NBS tables of chemical thermodynamic properties. Selected values for inorganic and C1 and C2 organic substances in SI units*. National Standard Reference Data System.

Wolery, T.W., Xiong, Y.-L., and Long, J. (2010) Verification and Validation Plan/Validation Document for EQ3/6 Version 8.0a for Actinide Chemistry, Document Version 8.10. Carlsbad, NM: Sandia National laboratories. ERMS 550239.

Wood, S.A., Palmer, D.A., Wesolowski, D.J. and Bénézeth, P.A.S.C.A.L.E., 2002. The aqueous geochemistry of the rare earth elements and yttrium. Part XI. The solubility of $Nd(OH)_3$ and hydrolysis of Nd^{3+} from 30 to 290ºC at saturated water vapor pressure with in-situ pHm measurement. *Water–rock interactions, ore deposits, and environmental geochemistry: a tribute to David Crerar, Special Publication*, *7*, pp.229-256.

Xiong, Y.-L. (2011a) WIPP Verification and Validation Plan/Validation Document for EQ3/6 Version 8.0a for Actinide Chemistry, Revision 1, Document Version 8.20. Supersedes ERMS 550239. Carlsbad, NM. Sandia National Laboratories. ERMS 555358.

Xiong, Y.-L., 2014. Sandia National Laboratories Waste Isolation Pilot Plant (WIPP) Analysis AP-155, Revision 3, Analysis Plan for Derivation of Thermodynamic Properties Including Pitzer Parameters for Solubility Studies of Borate. Carlsbad, NM: Sandia National Laboratories. ERMS 562807.

Xiong, Y., 2017. Solution Chemistry for Actinide Borate Species to High Ionic Strengths: Equilibrium Constants for $AmHB_4O_7^{2+}$ and $AmB_9O_{13}(OH)_4$(cr) and Their Importance to Nuclear Waste Management. *MRS Advances,* 2, 741–746.

Xiong, Y.-L., Domski, P.S., 2016. "Updating the WIPP Thermodynamic Database, Revision 1, Supersedes ERMS 565730." Carlsbad, NM: Sandia National Laboratories. ERMS 566047.

Xiong, Y.-L., and Lord, A.C.S. (2008) Experimental investigations of the reaction path in the $MgO–CO_2–H_2O$ system in solutions with ionic strengths, and their applications to nuclear waste isolation. Applied Geochemistry, 23, 1634–1659.

Xiong, Y.-L., Deng, H.-R., Nemer, M., and Johnsen, S. (2010) Experimental determination of the solubility constant for magnesium chloride hydroxide hydrate

403 ($Mg_3Cl(OH)_5 \cdot 4H_2O$), phase 5) at room temperature, and its importance to nuclear
404 waste isolation in geological repositories in salt formations. Geochimica et
405 Cosmochimica Acta, 74, 4605-46011.

406 Xiong, Y., Kirkes, L. and Westfall, T., 2013. Experimental determination of solubilities
407 of sodium tetraborate (borax) in NaCl solutions, and a thermodynamic model for the
408 Na-$B(OH)_3$-Cl-SO_4 system to high-ionic strengths at 25°C. *American Mineralogist*,
409 *98*(11-12), pp.2030-2036.

410 Zhang, X., Ma, H., Ma, Y., Tang, Q. and Yuan, X., 2013. Origin of the late Cretaceous
411 potash-bearing evaporites in the Vientiane Basin of Laos: δ 11 B evidence from
412 borates. *Journal of Asian Earth Sciences*, *62*, pp.812-818.

413 Zheng, M.-P., 1997. Classification of Saline Lakes and Types of Mineral Deposit. In *An*
414 *Introduction to Saline Lakes on the Qinghai—Tibet Plateau* (pp. 79-84). Springer
415 Netherlands.

416
417

Table 1. Experimental results produced in this study at 22.5 ± 0.5 ºC.

Experimental Number	Experimental time, days	pH_m*	Molal total Magnesium concentrations, $m_{\Sigma Mg}$, mol•kg^{-1}	Molal total boron concentrations, $m_{\Sigma B}$, mol•kg^{-1}	Molal total sodium concentrations, $m_{\Sigma Na}$, mol•kg^{-1}	Molal total chloride concentrations, $m_{\Sigma Cl}$, mol•kg^{-1}
SYN-Boracite	970	8.85	8.69E-01	5.21E-01	3.28E-01	1.74
	1217	8.90	8.52E-01	5.85E-01	3.26E-01	1.74
	1279	8.82	8.66E-01	6.03E-01	2.98E-01	1.75
	1302	8.83	8.63E-01	5.89E-01	3.30E-01	1.76
	1335	8.81	8.58E-01	5.66E-01	N/A [A]	1.76
	1483	8.82	8.58E-01	5.10E-01	N/A [A]	1.79
	1595	8.86	8.66E-01	4.88E-01	3.09E-01	1.79
	1642	8.87	8.74E-01	5.29E-01	3.20E-01	1.79

*pcH are first calculated based on pH readings and correction factors for $MgCl_2$ solutions from Hansen (2001), and then pcH are converted to pH_m based on the equation from Xiong et a. (2010). As the experimental solutions contain significant amounts of sodium and borate as well as the supporting medium, $MgCl_2$, the pH_m's calculated based on the correction factor for pure $MgCl_2$ might contain some additional experimental uncertainties. The uncertainties for pH_m by using the correction factor for pure $MgCl_2$ are estimated to be less than ± 0.08 according to the comparison with the correction factors for NaCl used in Xiong (2008) at the ionic strengths of the experiments in this work. In the thermodynamic calculations, the uncertainties include those for pH_m.

[A] In the corresponding EQ3NR input files, the sodium concentration at 1,302 days was used.

Table 2. Equilibrium constants at infinite dilution for boracite and aksaite at 25°C and 1 bar determined in this study.

Reaction	$\log_{10} K^0$ [A, B]
$Mg_3B_7O_{13}Cl(cr) + 15H_2O(l) \rightleftharpoons 3Mg^{2+} + 7B(OH)_4^- + Cl^- + 2H^+$	–29.50 ± 0.39 (2σ)
$MgB_6O_7(OH)_6{\bullet}2H_2O(cr) + 9H_2O(l) \rightleftharpoons Mg^{2+} + 6B(OH)_4^- + 4H^+$	–44.41 ± 0.41 (2σ)
$Mg_3B_7O_{13}Cl(cr) + 10H^+ + 11B(OH)_4^- \rightleftharpoons 3MgB_6O_7(OH)_6{\bullet}2H_2O(cr) + 12H_2O(l) + Cl^-$	103.90 ± 0.57 (2σ)

[A] The equilibrium constants were calculated based on all of the experimental data tabulated in Table 1. The uncertainty in terms of 2σ includes that for the small extrapolation from 22.5°C to the standard temperature of 25°C, using the equation, $\Delta G_T^o = \Delta G_{298.15}^o - (T - 298.15)\Delta S_{298.15}^o + \int_{298.15}^{T} \Delta C_p^o dT - T\int_{298.15}^{T} \Delta C_p^o d\ln T$, assuming that the heat capacity change is zero in this temperature range.

[B] Notice that the EQ3/6 files used for calculations of activities of H^+, Mg^{2+}, $B(OH)_4^-$, Cl^- and activities of water for extrapolation to infinite dilution, are internally, electronically archived under "/nfs/data/CVSLIB/WIPP_EXTERNAL/ap155/Files". It is conducted under Task 1 in AP-155 (Xiong, 2014).

Table 3. Equilibrium constants at infinite dilution for boracite and aksaite at 25°C and 1 bar calculated from the Gibbs free energies from the literature.

Reaction	$\log_{10} K^0$
$Mg_3B_7O_{13}Cl(cr) + 15H_2O(l) \rightleftharpoons 3Mg^{2+} + 7B(OH)_4^- + Cl^- + 2H^+$	–29.50 [A]
$Mg_3B_7O_{13}Cl(cr) + 15H_2O(l) \rightleftharpoons 3Mg^{2+} + 7B(OH)_4^- + Cl^- + 2H^+$	–30.61 [B]
$MgB_6O_7(OH)_6{\bullet}2H_2O(cr) + 9H_2O(l) \rightleftharpoons Mg^{2+} + 6B(OH)_4^- + 4H^+$	–44.95 [C]
$MgB_6O_7(OH)_6{\bullet}2H_2O(cr) + 9H_2O(l) \rightleftharpoons Mg^{2+} + 6B(OH)_4^- + 4H^+$	–57.80 [B]

[A] The equilibrium constant was calculated from the ΔG_f^0 from Khodakovsky, Semenov and Aksaenova (unpublished data, cited by Anovitz and Hemingway. 2002), consistent with the NBS Thermodynamic Tables (Wagman et al., 1982). In Khodakovsky, Semenov and Aksaenova, ΔG_f^0 was calculated from the ΔH_f^0 and S^0 data measured with the calorimetric method.

[B] The equilibrium constant was calculated from the estimated ΔG_f^0 from Anovitz and Hemingway (2002), consistent with the NBS Thermodynamic Tables (Wagman et al., 1982).

[C] The equilibrium constant was calculated from the estimated ΔG_f^0 from Li et al. (2000), consistent with the NBS Thermodynamic Tables (Wagman et al., 1982).

Table 4. Thermodynamic properties of aksaite and boracite at 298.15 K and 1 bar

Species	ΔH_f^0, kJ•mol^{-1}	ΔG_f^0, kJ•mol^{-1}	S^0 J•mol^{-1}•K^{-1}	References and Remarks
Aksaite	–6135	–5569	361	Anovitz and Hemingway (2002). See footnote A
Aksaite	–6063.65 ± 4.85	–5495.64	353.64	Jia et al. (1999). See footnote B
Aksaite	–6007.00	–5495.64	N/A	Li et al. (1999). See footnote C
Aksaite	–6063.65 ± 4.85	–5493.16 ± 2.16	346.69 ± 1.85	This work. See footnote D.
Boracite	–6575.0 ± 9	–6178.4 ± 9	253.6 ± 0.5	Khodakovsky, Semenov and Aksaenova (unpublished data, cited by Anovitz and Hemingway. 2002). See footnote E.
Boracite	–6565.3	–6184.7	307	Anovitz and Hemingway (2002). See footnote F.
Boracite	–6575.93 ± 2.03	–6179.25 ± 2.02	253.6 ± 0.5	This work. See footnote G.

[A] All properties were estimated.

[B] Enthalpy was experimentally determined. Gibbs free energy was calculated using the group contribution method of Li et al. (1999). Entropy was calculated from experimental enthalpy and estimated Gibbs free energy.

[C] All properties were estimated.

[D] Enthalpy is from the experimental value of Jia et al. (1999) using the calorimetric method. Gibbs free energy was computed from the experimentally determined equilibrium constant from this work. Entropy is calculated from the experimental enthalpy from Jia et al. (1999) and the derived Gibbs free energy from the experimental equilibrium constant from this work.

[E] Unpublished data from Khodakovsky, Semenov and Aksaenova using the calorimetric method (cited by Anovitz and Hemingway. 2002).

[F] All properties were estimated.

[G] Entropy is from the experimental value of Khodakovsky, Semenov and Aksaenova using the calorimetric method (cited by Anovitz and Hemingway. 2002). Gibbs free

energy was computed from the experimentally determined equilibrium constant from this work. Enthalpy is calculated from the experimental enthalpy from Khodakovsky, Semenov and Aksaenova using the calorimetric method (cited by Anovitz and Hemingway. 2002) and the derived Gibbs free energy from the experimental equilibrium constant from this work.

Figure Captions

Figure 1. XRD patterns of the solid phases in the experiments. Notice that the vertical lines in pink are the reference peaks of boracite, and the vertical lines in red are the reference peaks of aksaite. There are two reference standard for boracite. One is from the online database, RRUFF (http://rruff.info/), accessed on February 9, 2017, and the other is from the database of the International Centre for Diffraction Data, ICDD. The reference peaks for boracite from ICDD are represented by the vertical lines in pink, and the reference peaks for boracite from RRUFF are represented by the pattern in blue.

Figure 2. A plot showing experimental total boron, chloride, magnesium and sodium concentrations as a function of experimental time.

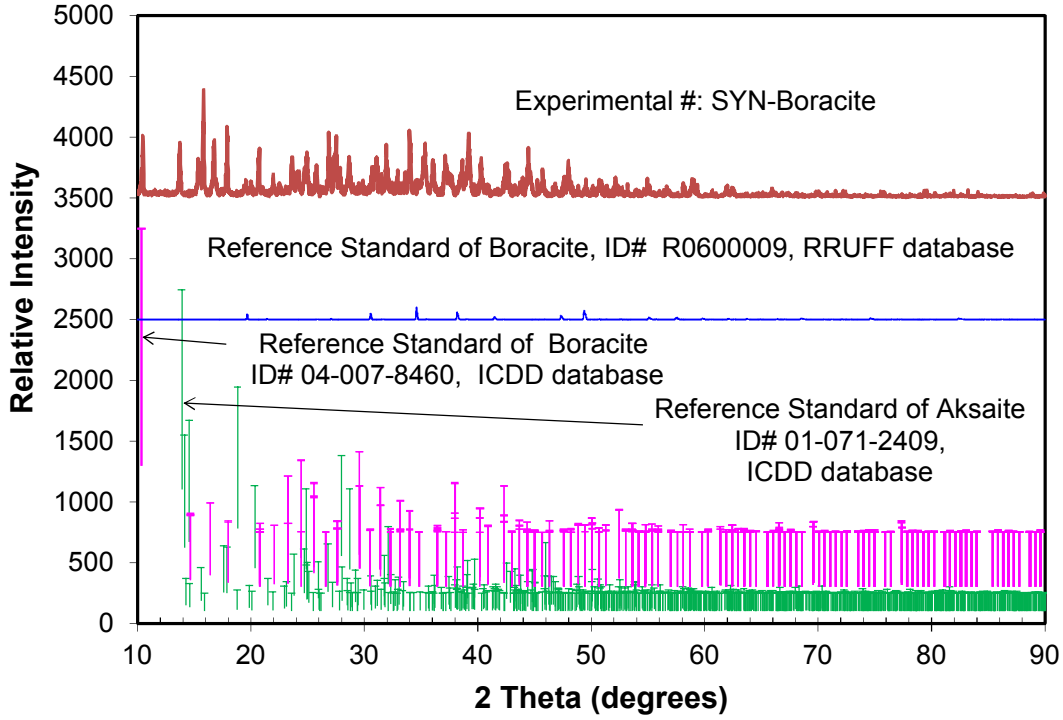
Relative Intensity
5000
4500
4000
3500
3000
2500
2000
1500
1000
500
0
10
20
30
40
50
60
70
80
90
2 Theta (degrees)
Experimental #: SYN-Boracite
Reference Standard of Boracite, ID# R0600009, RRUFF database
Reference Standard of Boracite
ID# 04-007-8460, ICDD database
Reference Standard of Aksaite
ID# 01-071-2409,
ICDD database

Figure 1.

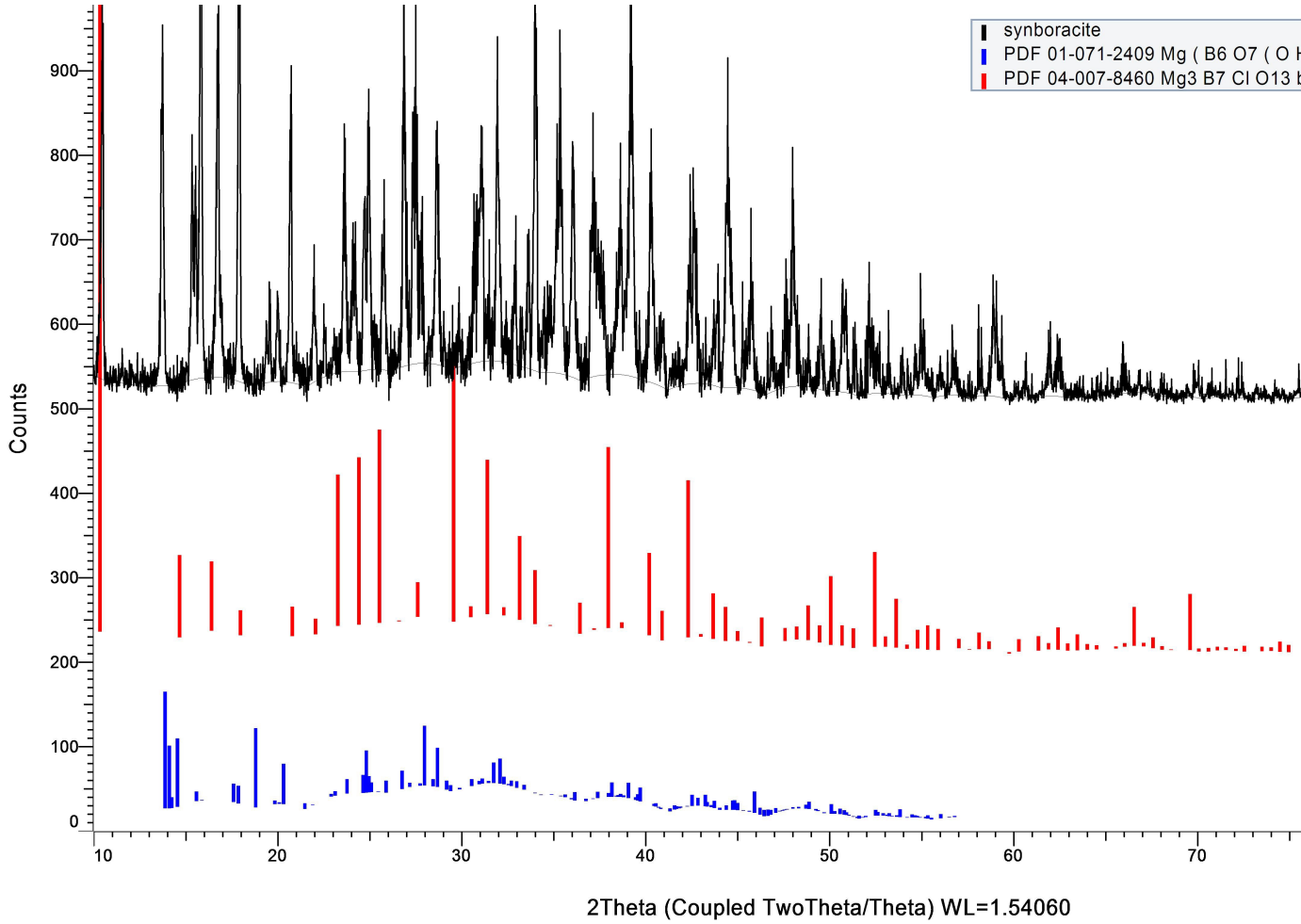

Figure 1. Duplicate

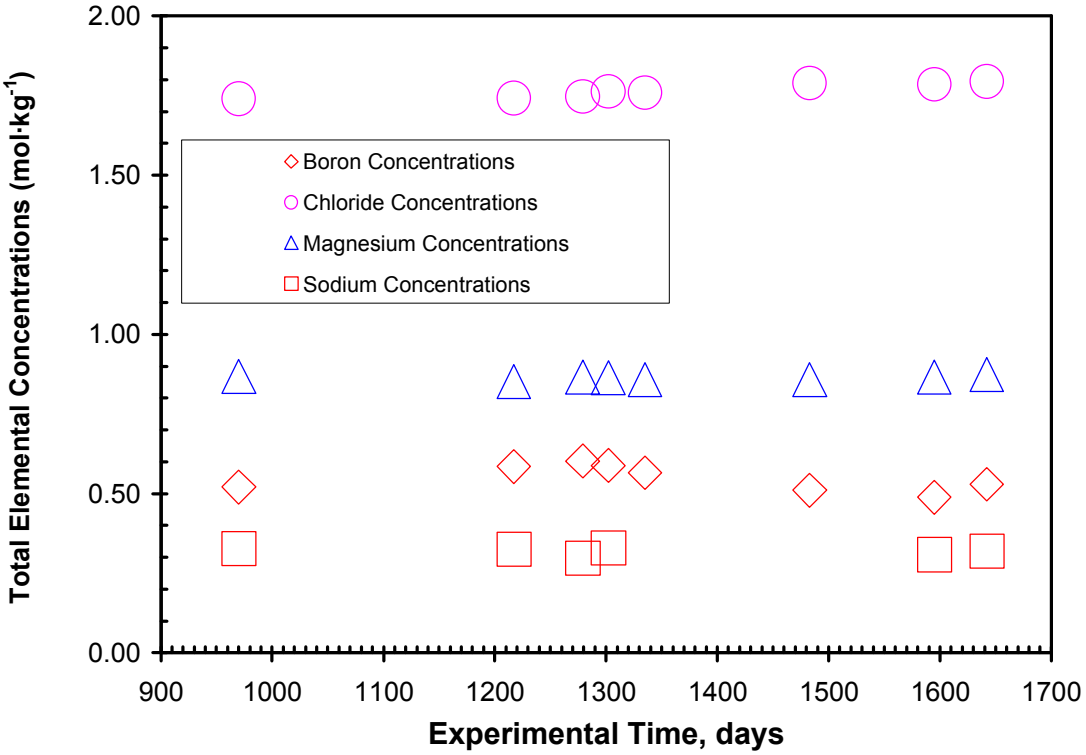
Total Elemental Concentrations (mol·kg-1)
2.00
1.50
1.00
0.50
0.00
900
1000
1100
1200
1300
1400
1500
1600
1700
Experimental Time, days
Boron Concentrations
Chloride Concentrations
Magnesium Concentrations
Sodium Concentrations

Figure 2.